

# Handling Qualities of Flexible Aircraft: from Modeling to Pilot-in-the-Loop Assessment

Jana Schwithal<sup>1</sup>, Christian Wallace<sup>2</sup>, Christoph Deiler<sup>3</sup> and Yasim Julian Hasan<sup>4</sup>

*Deutsches Zentrum für Luft- und Raumfahrt (DLR), Institute of Flight Systems, Braunschweig  
Germany*

Daniel Drewiacki<sup>5</sup> and Fernando J. O. Moreira<sup>6</sup>

*Embraer, São José dos Campos, Brazil*

Modern passenger aircraft designs are driven by ecological and economical constraints that require the aircraft to become more efficient and reduce their emissions. In order to achieve this, future aircraft designs are often characterized by light structures and high aspect ratios and consequently exhibit an increased aeroelastic flexibility. This increased flexibility can influence the handling qualities of the aircraft. Whereas classical flight dynamics assessments usually assume a rigid-body aircraft model, this assumption is not valid anymore for modern aircraft with increased aeroelastic flexibility. The eigenfrequencies of the structural modes are very low and can interact with the rigid-body dynamics and influence the pilots' perception and behavior. It is thus essential to include the aeroelastic effects in the aircraft model and consider their influence on the handling qualities. The present paper presents a way to a meaningful handling qualities analysis of a modern flexible passenger aircraft. This includes the model composition and system identification of flight test data, a handling qualities analysis of the developed model as well as the integration of the flexible model in a motion simulator and pilot-in-the-loop handling and PIO and ride qualities evaluations.

## I. Introduction

Striving for reduction in operation costs, fuel consumption and emission new aircraft designs are often characterized by high aspect ratios and light and slender wings of new composite structures. These aircraft configurations are very efficient and therefore highly desirable from a performance perspective, but they also show an increased aeroelastic flexibility, which poses new challenges in the aircraft design. One aspect is the influence of the enhanced flexibility on handling qualities of the aircraft.

Classical flight dynamic evaluations often do not account for the effects of aeroelastic flexibility. Previous studies [1] showed, however, that structural flexibility can introduce lags to the rigid-body dynamics and lead to the occurrence of Pilot-Induced Oscillations (PIO). It is thus essential to intensively study the handling qualities and especially tendencies to PIOs or involuntary inputs resulting from structural vibrations of these modern aircraft configurations. The traditional approach of analyzing the decoupled rigid-body low-frequency flight mechanics is not sufficient anymore. Whereupon for former aircraft designs the low-frequency rigid-body eigenmodes and the

---

<sup>1</sup> Research scientist, AIAA Member.

<sup>2</sup> Research scientist.

<sup>3</sup> Research scientist, AIAA Member.

<sup>4</sup> Research scientist.

<sup>5</sup> Product Development Engineer.

<sup>6</sup> Senior Flight Control Engineer, AIAA Member.

eigenfrequencies of the weak-elastic structure were clearly separated in the frequency bandwidth, modern aircraft are often characterized by very low structural eigenfrequencies, which interact with the rigid-body dynamics.

In order to receive a comprehensive handling qualities analysis of a modern aircraft, it is thus essential to include the aeroelastic effects in the flight dynamic assessment. The research project DinAFlex (Dynamics of Flexible Aircraft) of Embraer and the Institute of Flight Systems of DLR (German Aerospace Center) has the focus to investigate the influence of structural flexibility on the handling qualities of a modern passenger aircraft. This includes the development of a suitable flexible aircraft model, the application of handling qualities criteria and especially an extensive simulator study, in which test pilots evaluate the effects of the structural flexibility.

As the model development is driven by the requirement to perform a pilot-in-the-loop simulator campaign, virtual rigid-elastic models, which are able to represent the coupled and complex low-frequency dynamic behavior in real-time simulations, are necessary. Coupled large high-order aeroelastic FEM-CFD (finite element method-computational fluid dynamics) models are not applicable in a simulator campaign since time simulations are computationally extremely intensive. Instead, the low-order aeroelastic modeling approach suggested by [2] is applied here to achieve an efficient model of low complexity but sufficient accuracy for the handling qualities analysis. To ensure a realistic aircraft behavior, the model development harmonized with real measurement flight data by applying a system identification process to translate the measured aircraft dynamics into representative model parameters.

During the last years the DLR Institute of Flight Systems made first investigations concerning the identification of flexible airplanes, especially in terms of the coupling of low-frequency structural flexibility and general flight dynamics. This research was performed on a less complex aircraft system, precisely the DLR Discus 2C sailplane ([3]-[9]). For a passenger aircraft like the conceptual model of a regional jet considered in this paper, the structural dynamics are mass-case sensitive and strongly dependent on the current flight-point and thus require a more complex modeling approach. The present paper extends the methods of the previous work for the application to a conceptual modern regional jet with the purpose to evaluate the handling qualities of this aircraft.

As the influence of structural flexibility is like to further increase for future aircraft, the DinAFlex project also studies the effects for further increased flexibility. For this purpose, a conceptual aircraft model with artificially reduced structural stiffness is included in the analysis and also evaluated in the pilot-in-the-loop simulations.

## II. Modeling Approach

The identification and simulation of the flexible passenger aircraft is based on the model formulations presented in this section. The structural dynamics of the elastic aircraft body are represented through a system of decoupled linear ordinary differential equations of motion, including the modal displacements and the modal accelerations of the elastic mode shapes. The formulation of the aerodynamic model part is a combination of a nonlinear and a linear derivative model. The non-linear derivative model represents the aerodynamic characteristics of the basic rigid-body aircraft. This assumption is supposed to be valid within the complete flight envelope. The linear aerodynamic derivative model represents the changes of the aircraft aerodynamics induced by flight-point dependent shape deviations of the elastic aircraft structure. The coupling between the six-degree-of-freedom (6-DoF)-rigid body dynamics and the (M-DoF)-structural dynamics is realized by implementing distinct coefficients in the aerodynamic modeling approach in each model part.

### A. Model Formulation

The nonlinear rigid aircraft dynamics are modeled by a standard 6-DoF model on the basis of the gravitational, engine and aerodynamic forces and moments. The nonlinear rigid-body (6-DoF) aircraft aerodynamic model is formulated as a two-point model, splitting up the wing and horizontal tailplane influences [10]. The aerodynamic model is based on the well-established derivative model formulation mainly used in DLR for system identification purposes, as described in detail, for instance, using the example of the model of the former DLR in-flight simulator VFW 614 ATTAS, which is given in [11] as a result a system identification process.

The extension of a rigid-body aircraft simulation model regarding the flexible dynamics allows to simulate the complete dynamic aircraft behavior including the deformation of fuselage, wing and empennage as well as the cross-coupling in between rigid and flexible dynamics. The necessary model formulations for the coupled aircraft simulation are given for example by Waszak and Schmidt in [2].

The dynamics of an elastic and discretized structural mechanical system, which is used here for the extension of the nonlinear rigid-body model approach, can be described via a linear system of ordinary differential equations. Using modal mass matrix  $\mathbf{M}_\phi$ , the modal stiffness matrix  $\mathbf{K}_\phi$ , modal displacement  $\boldsymbol{\eta}(t)$  and its derivatives, and generalized loads  $\mathbf{Q}(t)$ , the equations of motion for an excited elastic undamped structure can be expressed as

$$\mathbf{M}_\Phi \cdot \ddot{\boldsymbol{\eta}}(t) + \mathbf{K}_\Phi \cdot \boldsymbol{\eta}(t) = \mathbf{Q}(t). \quad (1)$$

In consideration of the normalized form, each mode shape-related differential equation is equivalent to an independent Single-Degree-of-Freedom (S-DoF) system given by

$$\ddot{\eta}_i(t) + \omega_{0,i}^2 \cdot \eta_i(t) = \frac{Q_i(t)}{m_{\Phi i}} = Q_i(t), \quad i = 1 \dots N, \quad (2)$$

whereupon the eigenvectors are scaled in that way that the modal mass  $m_{\Phi i}$  is equal to one, such that

$$\omega_{0,i}^2 = \frac{k_{\Phi i}}{m_{\Phi i}} = k_{\Phi i} \quad (3)$$

represents the mode shape related eigenfrequency.

The interconnection between the rigid and the structural dynamic description of the aircraft behavior is provided by the modeling of the aerodynamic forces and moments, including an extended set of model parameters. The individual external generalized load  $Q_i$  in equation (2), which represents the summation of all external influences that excite the individual flexible mode shape, is thereby split in two parts:

$$Q_i(t) = Q_{i,\text{RB}}(t) + Q_{i,\text{Flex}}(t). \quad (4)$$

$Q_{i,\text{RB}}$  contains all excitations of the flexible modes resulting from the general aircraft motion and the effects resulting from control surface deflections, including an additional part  $\Delta Q_i$ , which might contain miscellaneous influences such as atmospheric disturbances.  $Q_{i,\text{Flex}}$  represents the generalized (aerodynamic) loads that are induced by the aerodynamic feedback of the elastic mode shapes.

Note that modal damping is not modelled as explicit structural modal damping, but implicitly considered in this modeling approach by the influence of the modal velocities  $\dot{\eta}_i$  on the generalized loads  $Q_i$  (in  $Q_{i,\text{Flex}}$ ).

In the system identification and the further analysis of the model, the flexible model is often divided into a quasi-static and a dynamic part. This is based on the approach that the modal displacements  $\eta_i$  are divided into a quasi-static (QS) and dynamic part as

$$\eta_i(t) = \eta_{i,\text{dyn}}(t) + \eta_{i,\text{QS}} \quad (5)$$

whereupon  $\eta_{i,\text{dyn}}$  represents the aircraft's elastic structural oscillation around a distinct flight point dependent quasi-static modal deflection  $\eta_{i,\text{QS}}$ . This quasi-static displacement is (in relation to a non-deformed basic rigid aircraft) equivalent to an offset-deflection to reproduce the flight shape [12]. If only quasi-static parts of the model are considered ( $\eta_{i,\text{dyn}}(t) = 0$ ), it is still a flexible aircraft model, but the dynamic transients are not considered. By definition the derivatives of the quasi-static are zero:

$$\dot{\eta}_{i,\text{QS}} = \ddot{\eta}_{i,\text{QS}} = 0. \quad (6)$$

## B. Modal Alignment

To consider the impact of flexibility on the flight dynamics sufficiently and to keep the size of the model as small (and computationally efficient) as possible, the implemented structural data is limited to the elastic mode shapes located in the lower frequency bandwidth. This modal truncation suppresses the possibly occurring effects of elastic mode shapes of higher order, which are here at the same time supposed to be very small and therefore negligible.

In order to investigate the influence of specific elastic mode shapes on the parameter estimation processes and afterwards on the handling qualities, a modal alignment process is applied. This means that the individually implemented modal sequence is aligned for each used mass case (mass distribution) and flight point in relation to a globally predefined modal reference sequence. The identified parameters are thus driven by (nearly) identical modal characteristics, if the model is extended sequentially by adding full structural dynamics of a single elastic mode shape in a step-by-step model extension process. For the handling qualities analysis this modal alignment process ensures that the influence of a specific elastic mode shape on a system parameter is nearly identical for all available mass cases and flight points. This simplifies the analysis of the influence of different elastic modes on the handling qualities analysis and flight dynamics behavior.

Figure 1 exemplarily shows the general principle of the modal alignment process. Flexible modes are traditionally ordered by increasing frequency, as illustrated on the left-hand side of Fig. 1. This implies that different mass cases usually exhibit a different order of their physical modes, e.g. the first torsional mode can be the third mode for mass configuration 1 and the second mode for mass configuration 2. To allow an interpretation of the physical influence of specific modes the modes are rearranged in a new so-called reference sequence (right-hand side of Fig. 1), in which

modes with the same physical characteristics, i.e. the same mode shape type, always occur as the same mode in the sequence, e.g. the first torsional mode is always the third mode for all mass cases. The quantity of the specific mode shape type as well as the existing types can thereby vary for different mass configurations. Furthermore, the exact frequency at which a specific mode shape occurs can be different for different mass configurations as well. The red line marked with “f1” in Fig. 1 exemplarily indicated a cutoff frequency to illustrate this effect. It can be noticed that for mass case 1 four modes are lower than the cutoff frequency f1, whereupon for mass case 2 five elastic modes are included below this frequency. In the present project the cutoff frequency was selected as 10 Hz. Modes at higher frequencies are not included in the model. The reason for this was at the one hand that their influence in the handling qualities is considered to be negligible and on the other hand the simulator is not able to reproduce frequencies above 10 Hz.

Due to the variances in the different mass configurations it is usually not possible to achieve a modal matching of the mode shapes for all given modes. Instead, only a fixed number of modes (four in Fig. 1) are ordered according to their mode shape type for all mass cases. This represents the mass-case-independent mode sequence. The remaining modes are included in a mass-case-dependent sequence and vary in their order for different mass configurations.

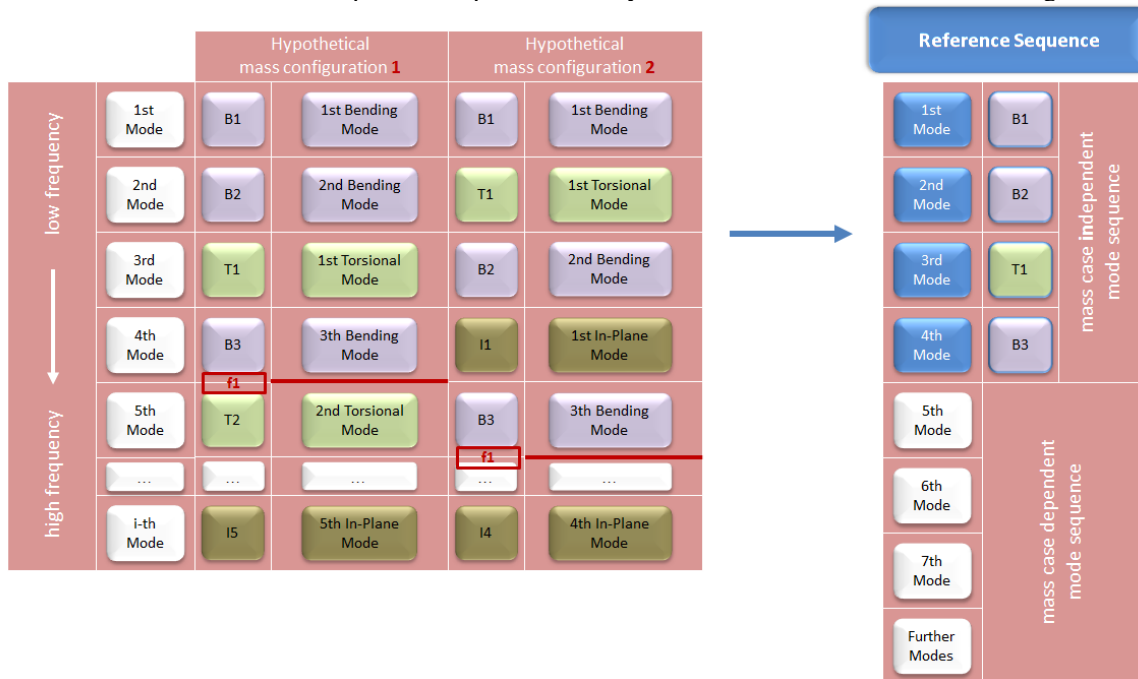


**Fig. 1 Schematic representation of modal alignment process.**

The modal alignment is realized by applying the modal assurance criterion (MAC). This criterion, described in detail in [13], evaluates which mode shape is similar to another mode shape of another mass case by comparing the eigenvectors of the solution of the generalized eigenvector problem of two mass cases (considering a non-conservative structural dynamic system as implemented and described above). The MAC value approaches one the more two mode shapes correspond to each other. The comparison of a mode shape against itself would thus provide a diagonal with ones in the MAC. Figure 2 illustrates the modal assurance criterion for the comparison mass case A and B in their original mode shape sequence (a) as well as the modified mass cases with the permuted mode order after the alignment process. In the reordered case the first 5 flexible modes exhibit values close to 1 on the diagonal indicating that these mode shapes are very similar. This means that their modal characteristics are almost the same. When these reordered mode shapes are used for the handling qualities analysis later on, the physical characteristics of each mode shape are thus comparable for different mass cases. The influence of mode shape 3 of mass case A and mode shape 3 of mass case B, for instance, are nearly identical. Without the alignment process, the influence of one mode shape of two different mass cases would not be possible as the modal characteristics could be completely different for the different mass cases.

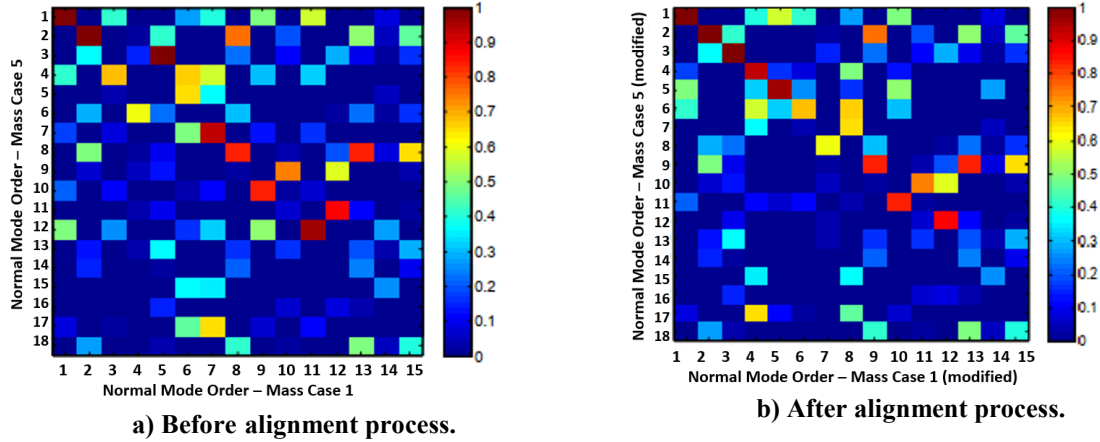


**Fig. 2 Comparison of two mass cases via modal assurance criterion.**

Table 1 displays the resulting new mode sequence for the mass cases 1 to 5 for the first 18 flexible modes. Rigid body modes are neglected here such that mode 1 represents the first flexible mode. The columns of each mass case indicate from which mode of the original mode sequence (ordered according to rising frequency) the present mode originates. Mode 3 of the new mode sequence for instance corresponds to mode 5 of the original order of mass case 1 and mode 3 of the original order of mass cases 2 to 5. The first 5 modes in Table 1 are mass-case-independent and show overall modal matches representing the reference sequence, i.e. they exhibit the same mode shape types for all five mass cases. These mode shapes types occurred at different positions in the original modal order. That is why they have different numbers for the different mass cases. But they exhibit almost the same physical characteristics, which is relevant for the new mode sequence after the modal alignment process.

The first 8 modes of the new mode sequence (marked in blue in Table 1) are implemented as full-dynamic modes and the ninth to 14th mode (marked in green in Table 1) are modeled as quasi-static modes. Higher modes are not included in the aircraft model for the handling qualities analysis, since their influence on handling qualities can be considered as negligible.

**Table 1 New mode sequence after alignment process (with mode 1 – 8 implemented **full-dynamically** and mode 9-14 **quasi-statically** in the new mode sequence)**

	new mode sequence	mass case 1	mass case 2	mass case 3	mass case 4	mass case 5
Mass-case-independent	1	1	1	1	1	1
	2	2	2	2	2	2
	3	5	3	3	3	3
	4	7	7	7	7	7
	5	11	12	12	12	12
Mass-case-dependent	6	3	4	4	4	4
	7	4	5	5	5	5
	8	6	6	6	6	6
	9	8	8	8	8	8
	10	9	9	9	9	9
	11	10	10	10	10	10
	12	12	11	11	11	11
	13	13	13	13	13	13
	14	14	14	14	14	14
	15	15	15	15	15	15
	16	-	16	16	16	16
	17	-	17	17	17	17
	18	-	18	18	18	18

The mass cases in this reordered new sequence represent the basis for the system identification process. The modal alignment allows to include flight test data with different mass cases in the overall system identification process whereupon the different modes are iteratively included. While reordering the structural modes during the modal alignment process, the related aerodynamic cross-coupling parameters thereby have to be reordered correspondingly.

### C. Modified Flexibility

The goal of this work was to evaluate general effects of structural flexibility on the handling qualities of aircraft. The analyses should thus exceed the assessment of today’s aircraft and also provide insights about potential future aircraft configurations with further increased flexibility. For this purpose, an additional generic model aircraft with reduced structural stiffness was generated. For the sake of simplicity this model will be called “extended flexible” model in the following. Note, however, that this model is not derived from a physical model with increased flexibility but that only the structural stiffness is artificially reduced by 50% from a conceptual model of a reginal jet. The (mass-normalized) modal stiffness matrix  $K\Phi$  is thus modified as

$$\omega_{0, Flex2} = 0.5 \cdot \omega_{0, Flex1}. \quad (6)$$

All other model parameters including the aerodynamic coefficient remain unchanged.

## III. Identification Process

The system identification process of a flexible aircraft is no easy task especially if there is a distinct focus on the validation of the model behavior including flight data for handling qualities evaluations and simulator experiments. There has been done some work related to this topic recently within DLR ([3]-[9]). The corresponding experience gained during the identification of flexible sailplane models is transferred to this work project and the identification strategy described hereafter.

The necessary four pillars for a successful system identification are described by the “Quad M” approach [14]. These pillars are:

- Maneuver: optimized system input for the distinct system identification task
- Measurement: high quality data sets containing the system response and all necessary observations for identifying the system structure
- Method: parameter estimation method applicable to the system identification task with regards to the overall objective
- Model: system model well representing the dynamic system physics

Within this work the model formulation described above was used because it suits the “Quad M” requirement. For model parameter estimation, the output-error in time domain (see section IV.A) was applied, because it provided good results in the previous projects ([3]-[9]) and has some advantages for the simulator model development in terms of model accuracy. A challenge for the model identification of the present model was the already existing flight data base, which mainly contains data of maneuvers from test flights which were not dedicated for system identification of flexible aircraft. Consequently, these maneuvers are not optimally designed for the identification task. Also, not all necessary observations are available during all flights. Hence, the strategy for the identification process in this case was to literally built a bridge over the two not perfectly shaped pillars “Maneuver” and “Measurement” of the “Quad M” approach.

### D. System Identification of Flexible Aircraft

Due to the increased structural flexibility of the considered aircraft, the excitation of low-frequency normal mode shapes during flight via commanded maneuvers or external disturbances possibly lead to large shape deviations of the structure in comparison to a supposed (unvarying) reference shape of a rigid body. This reference shape and its aerodynamic capabilities are up to now the presumed model structure in system identification of aircraft dynamics. The occurring structural deformations of the aircraft shape (resulting in the so-called flight shape) might accompany changed aerodynamic capabilities or influence the handling qualities of the aircraft in general if the elastic mode shapes and the rigid body eigenfrequencies are located close to each other in a small frequency bandwidth.

The geometric difference between the reference body shape and the flight shape is illustrated in Fig. 3 relating to the quasi-static wing deformation. The reference body shape and its inherent aerodynamic properties are represented by the limited parameter setting of the classical (6-DOF) nonlinear rigid model structure, which is commonly used in

flight dynamics. This rigid-body of the wing is displayed as the black straight line in Fig. 3. Naturally, this approximation of the airplane dynamics is not able to represent structural deformation because necessary structural degrees of freedom are not included in this modeling approach. In consequence, using this approach does not allow to consider the effects of aircraft shape deviations around the reference shape.

It is assumed that adding the influence of the quasi-static structural deformation related of different distinct elastic mode shape to the identified model will raise the capability of the resulting model structure to represent the (quasi-static part of the) measured flight shape. As only quasi-static deformation is considered here, this means that accelerations resulting from structural deformation, i.e. the dynamic transients to reach the quasi-static deformation is not included at this point. The model order is thereby increased piecewise via adding a single modal degree of freedom in each enlargement step. The blue, purple and orange line illustrate this exemplarily for 1, 2 and N modes of the quasi-static aeroelastic (QSAE) wing shape. If enough flexible modes are included, the resulting model represents the (quasi-static part of the) deformation during flight and the orange line in Fig. 3 matches (nearly) with the measured flight shape (green line). Note that there might still be measurement errors which lead to small deviations between the real flight shape and the measured flight shape.

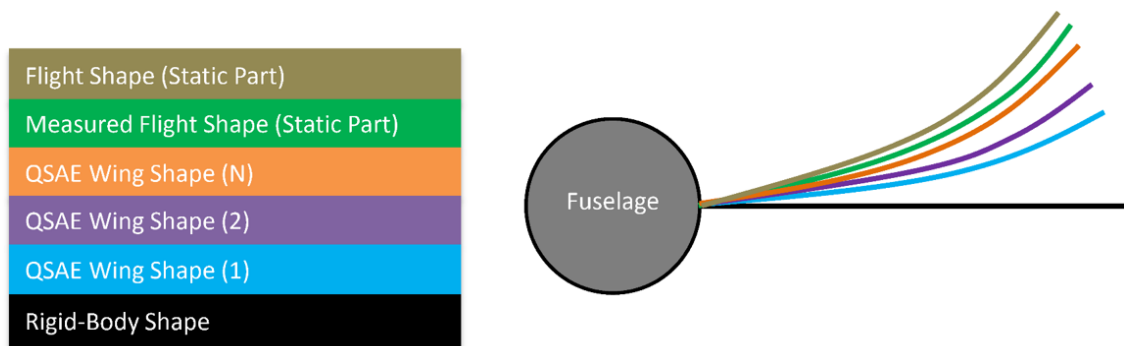


**Fig. 3 Example of different wing shapes when considering distinct effects in a steady flight condition.**

As in classical system identification of flight dynamics the first step is to identify a suitable set of parameters for the 6-DOF dynamic model, mainly the aerodynamic model part. The next step is to estimate the corresponding model parameters using a state-of-the-art parameter estimation technique like the output-error method in the time domain. Using data of an apparently flexible aircraft for this 'classical' identification without any model parts covering the structural dynamics might result in a less satisfying match of simulation results with the flight data and larger residuals containing the model deficiencies. Furthermore, some feedback from the local flexible motion of the structure to the global 6-DOF dynamics might be blurred into the identified 6-DOF-related aerodynamic parameter set. Note that during the identification process a best possible mathematical match of the model with the available data is obtained, even if this results in physically erroneous parameter values trying to represent the overall aircraft characteristics.

### E. Strategy for System Identification Process

The main hypothesis for the model system identification was that the available (predetermined) information about the aircraft's flexible dynamics – flight condition and mass-case-dependent linear structural dynamics models – are correct and the corresponding six-degree-of-freedom aircraft dynamics must be identified to cover the overall aircraft behavior (rigid and flexible). Consequently, the identification strategy must allow to determine the “missing” six-degree-of-freedom aerodynamics.

The identification process is split in two main parts. The first part of the iterative process is to estimate the parameters of the 6-DOF-aircraft under the quasi-static influence of flexible modes. Fig. 4 illustrates the first part of this process. The initial step for the cascading identification process is similar to the classical system identification process of aircraft dynamics using the basic nonlinear 6-DOF-model structure without any modal extensions. It is assumed that the results in terms of the calculated values of the basic parameter set can only represent a limited part of the overall aircraft dynamics. The actual process of flexible aircraft model identification can be started as a second step. The quasi-static influence of the different flexible modes is subsequently included in the identification process. Each time, when adding the quasi-static part of one mode, the parameters of the 6-DOF-aerodynamics must be estimated again to compensate the quasi-static elastic feedback on the rigid-body motion.

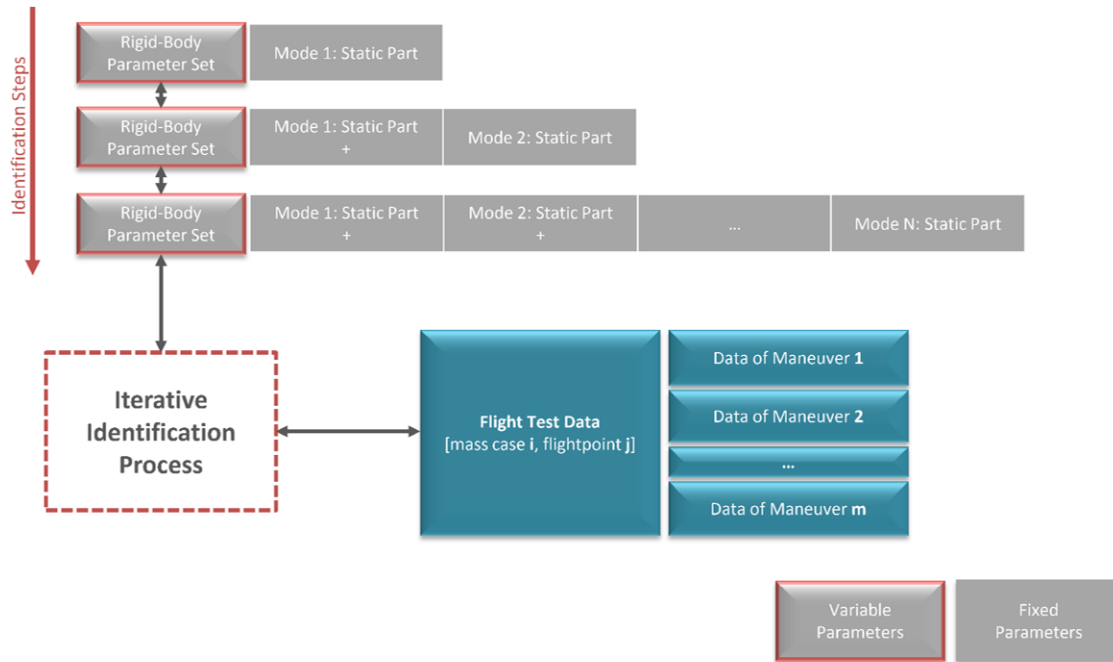


**Fig. 4** First part of iterative identification process: quasi-static influence on rigid-body aerodynamics.

By including the influence of an individual normal mode shape the updated and enlarged model (structure) will potentially allow to achieve a better predict of the measured aircraft response in the data. Hence, in the first identification step some parts of the model response were compulsorily assigned to the 6-DOF-motion characteristics, now this part of the response is correctly included in the model part representing the dynamics of the first normal mode shape. Until now some dynamics which are related to the elastic structural behavior that could not be covered by the limited parameter set of the basic 6-DOF-model, are now covered by the enlarged model.

Figure 5 shows the evolution of the rigid-body aerodynamic parameters during the iterative inclusion of more quasi-static modes in the estimation process using the example of the zero-lift coefficient  $C_{L0}$  as well as the lift curve slope  $C_{L\alpha,FW}$  and pitch damping coefficient  $C_{mq,FW}$  of the fuselage and wing. The evolution demonstrated the impact of the different quasi-static modes in the rigid-body aerodynamic parameters. The zero-lift coefficient and lift curve slope, for instance, are significantly influenced by the first four considered modes and do not vary very much anymore when the influence of further quasi-static modes is considered. The pitch damping coefficient changes during each iterative step during the process. With 14 quasi-static modes included in the identification process convergence could be achieved for most aerodynamic parameters. The order of the modes always corresponds to the new mode sequence after the modal alignment process (cf. Section B).

The second part of the iterative identification process is to account for the full flexible dynamics. On the basis of the result of the first part of the identification process, parts of flexible structural modeling that go beyond a purely quasi-static influence of the different modes are now subsequently included in the identification process, as illustrated in Fig. 6.

This second part of the process also shows the modulus approach for the simulation. The model resulting from the first part of the identification process is from this point on defined as the rigid-body simulation for further identification and simulation because removing the quasi-steady model parts will result in an erroneous model response. After adding step-

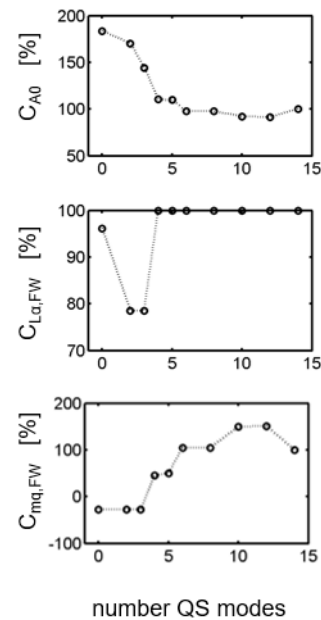


**Fig. 5** Example on evolution of rigid-body aerodynamic parameters with quasi-static modes.

by-step flexible modes' dynamics, the so-called intermediate flexible models are generated. These models also account for dynamic parts of distinct elastic mode shapes and the quasi-static corrections of all considered flexible modes  $N$ . The foreseen system identification process does include the estimation of certain rigid-body aerodynamics parameters as well as an adaption of specific coefficients of the flexible model part. This iterative process will finally lead to a validated model formulation including quasi-static corrections of  $N$  modes and account for the full dynamics of  $k$  modes (with  $k < N$ ). In the present project the quasi-static corrections of 14 modes and the full dynamics of 8 modes are considered.

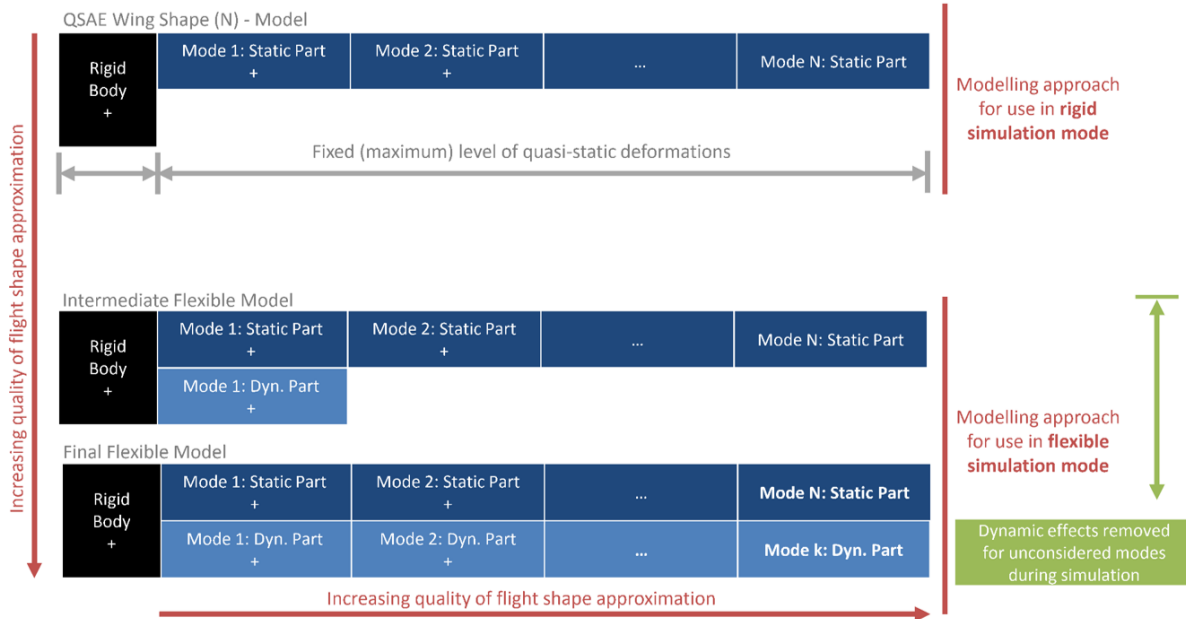


**Fig. 6 Second part of iterative identification process: quasi-static and fully dynamic influence on rigid-body aerodynamics.**

## F. Identification Results

The strategy for the system identification described above was applied to derive the (rigid-body) aerodynamic model, which will be used in combination with the given structural model to form the overall simulation model of the flexible aircraft. The following figures describe the match of the identified model with flight test data. The simulation model comprises 8 dynamic and additional 6 quasi-static flexible modes as described above. As already mentioned the available flight test data was not explicitly gathered for the purpose of system identification of the flexible aircraft model. The flight test data base contains measurements of all relevant signals for a 6-DoF model identification (considering flexible dynamics). For distinct flights also, measurements of accelerometers distributed along the aircraft's fuselage, wings and empennage were available. Unfortunately, these local acceleration measurements were not available for all flight test maneuvers necessary to perform the complete system identification. The local accelerations are not weighted within the parameter estimation process, but they are compared to the simulated values provided by the resulting model after the system identification.

Figure 7 exemplarily shows the comparison of the flight test data with the simulated aircraft model for the three maneuvers rudder doublet, bank angle change and a 3-2-1-1 elevator input. The aircraft dynamics are thereby simulated as rigid-body dynamics but the influence of the structural flexibility on the aerodynamics (modelled via the generalized loads  $Q_{i, Flex}$  as described in equations (2) and (4)) is considered for 8 fully dynamic and 6 quasi-static flexible modes. All displayed values are considered at the position of the inertia reference unit (IRU). It can be noticed that the simulation matches the flight data quite well. Small deviations can be seen at the very beginning of the maneuvers. These result from small offsets of the initial values of the modal displacements, which were necessary to achieve a stable simulation. The effects for the dynamics are, however, negligible and simulated dynamics show a good consistence with the flight data.

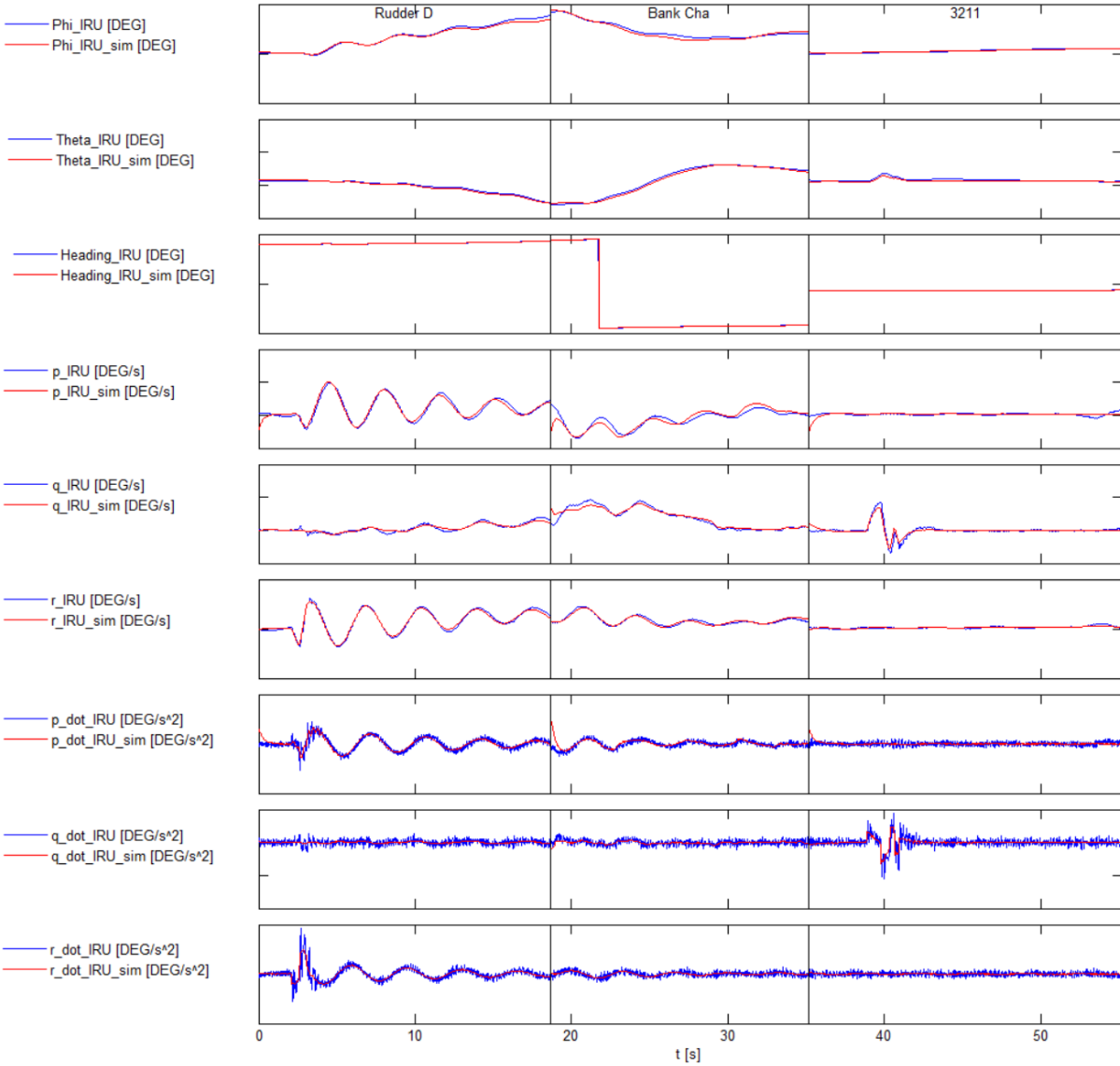


**Fig. 7 Example of match flight test data and simulated model for attitude and rotational rates.**

Figure 8 shows the accelerations measured by the inertia reference unit in flight (blue line) compared to the accelerations of the rigid-body model (red line) as well as with the fully dynamic model (green line). The rigid-body model displayed in red corresponds to the same modeling approach as in Fig. 7 with rigid-body dynamics including flexible aerodynamics, i.e. the simulated accelerations are transformed to the IRU position assuming a rigid aircraft structure with a constant lever-arm to the center of gravity. The fully dynamic model displayed in green also includes the structural dynamics itself and thus the flexible displacement of the IRU position given by the structural dynamics model. The closer zoom of the oscillations in Fig. 9 and Fig. 10 reveals that the inclusion of the flexible modes dynamics leads to an inclusion of higher-frequency oscillations in the simulation model and to a better match of the accelerations. The comparison to the flight data thus proves an acceptable match of model response with measured aircraft response. The measurement is not perfectly met but the dynamic model (green line) qualitatively reproduces the high-frequency oscillations with the correct frequency. To receive a better match, the parameters of the structural model (not only the aerodynamic parameters) would have to be adjusted. This would require more flight test data, which was not available in this project. As the pilot is not able to detect small deviations in the time response at these high frequencies, the given model is considered to provide an acceptable match of model response with measured aircraft response for the present analyses.

This fully dynamic modeling approach (green line) is used for the subsequent handling qualities analysis. The motion at the pilot seat, which is relevant for the handling qualities analysis and the simulator studies, is determined using the structural dynamics model providing the flexible displacement of the cockpit position.

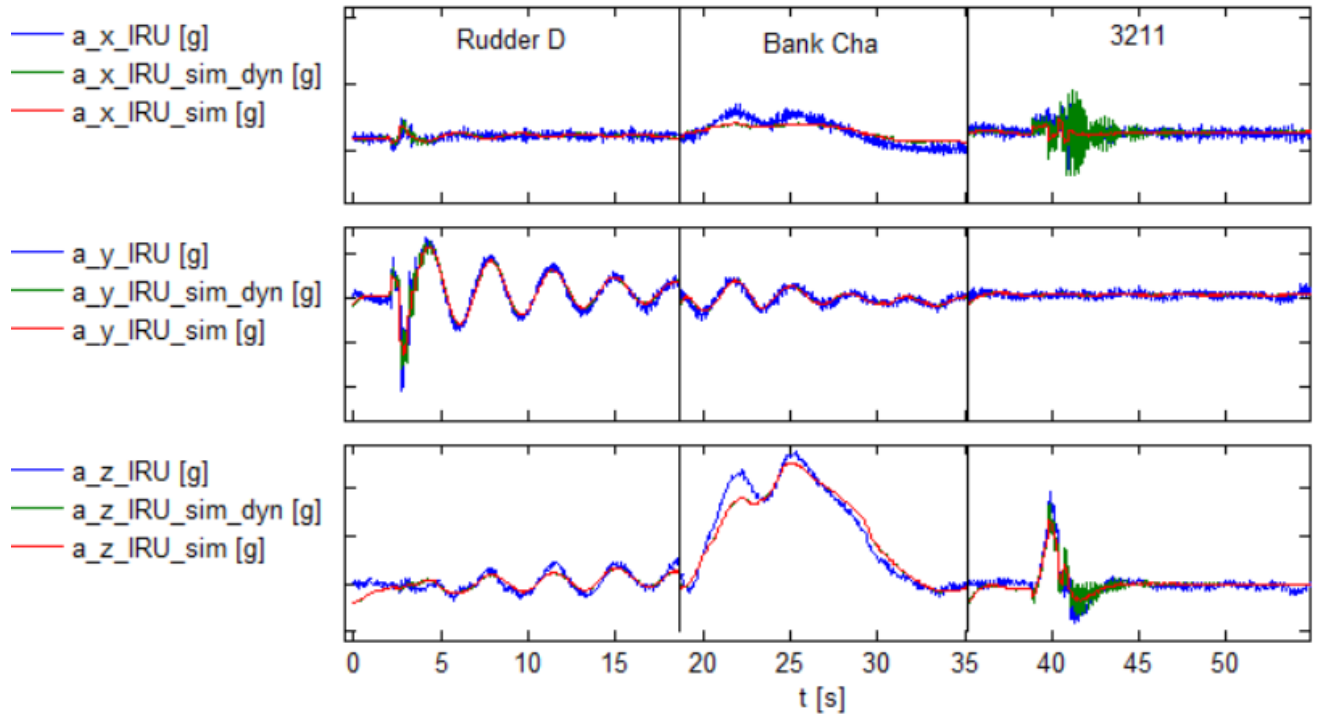


Fig. 8 Local accelerations with flexible dynamics influence.

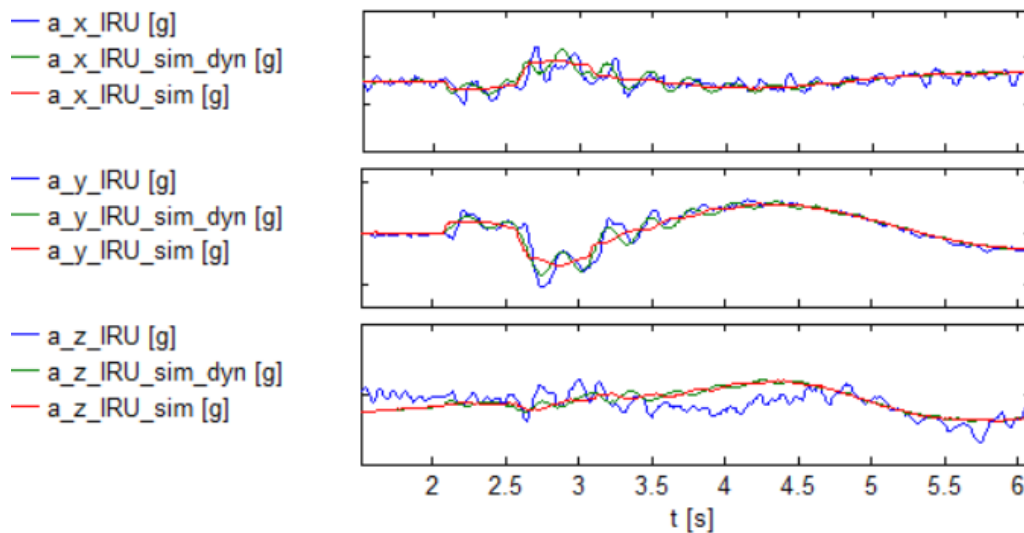


Fig. 9 Zoom of local accelerations with flexible dynamics influence in rudder doublet maneuver.

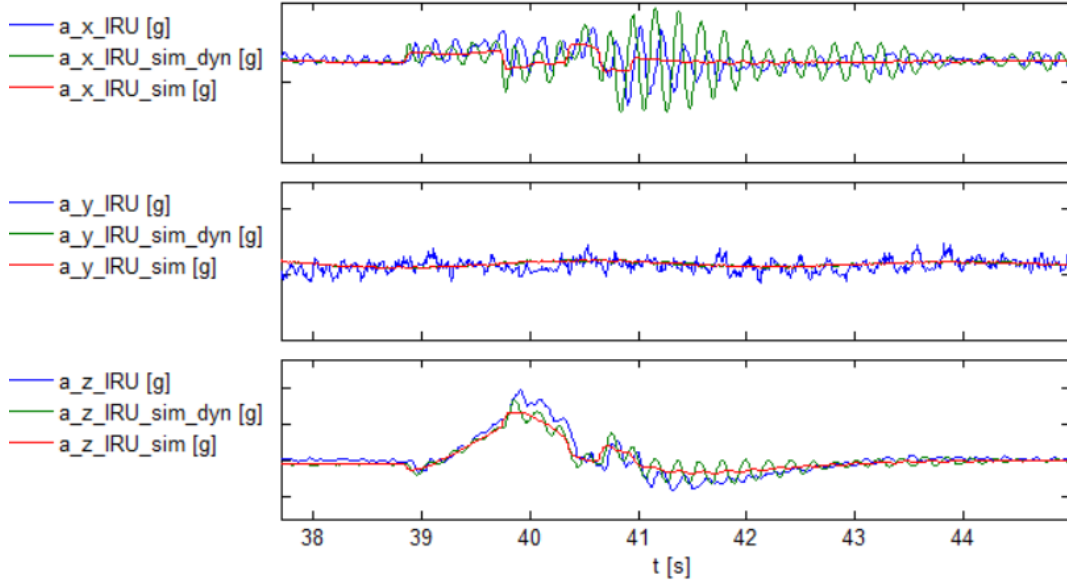


Fig. 10 Zoom of local accelerations with flexible dynamics influence in 3-2-1-1 elevator maneuver.

#### IV. Time Responses of the Identified Flexible Model

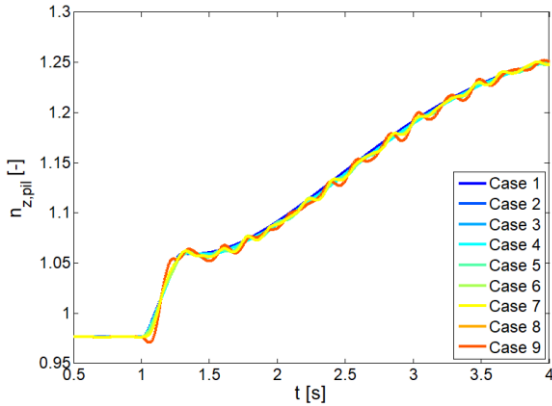
Before selected handling and riding qualities results are presented in the next section, this section provides some qualitative insights into the dynamics of the afore-presented identified model. In doing so, different combinations of activated and deactivated modes are simulated to show the impact of single flexible modes. As described in section III, the model is only valid for the flexible configuration it was identified for, i.e. 14 modes are included with their quasi-static parts and, in addition, the flexible dynamics of the first 8 modes are included. However, this approach serves well to show the effect, different modes' dynamics have on the aircraft behavior. Table 2 summarizes the different combinations along with their case names as used in this section. As shown, for the different cases, the respective modes are activated consecutively, which is in accordance with the process with which the model was identified.

Table 2 Definition of mode cases used in this section.

Case Name	Mode 1	Mode 2	Mode 3	Mode 4	Mode 5	Mode 6	Mode 7	Mode 8	Modes 9 - 14
Case 0	QS	QS	QS	QS	QS	QS	QS	QS	QS
Case 1	QS + flex	QS	QS	QS	QS	QS	QS	QS	QS
Case 2	QS + flex	QS + flex	QS	QS	QS	QS	QS	QS	QS
Case 3	QS + flex	QS + flex	QS + flex	QS	QS	QS	QS	QS	QS
Case 4	QS + flex	QS + flex	QS + flex	QS + flex	QS	QS	QS	QS	QS
Case 5	QS + flex	QS + flex	QS + flex	QS + flex	QS + flex	QS	QS	QS	QS
Case 6	QS + flex	QS + flex	QS + flex	QS + flex	QS + flex	QS + flex	QS	QS	QS
Case 7	QS + flex	QS + flex	QS + flex	QS + flex	QS + flex	QS + flex	QS + flex	QS	QS
Case 8	QS + flex	QS + flex	QS + flex	QS + flex	QS + flex	QS + flex	QS + flex	QS + flex	QS

With respect to both numerical handling qualities, such as for instance the C\*-criterion, and motion-simulator-based handling qualities assessment, the load factors at the pilot seat play a very important role. In order to demonstrate the influences of the flexibility on the dynamic behavior of the model, Fig. 11 shows the vertical load factor at the captain seat for an elevator nose-up step input and Fig. 12 shows the lateral load factor at the same location for a

rudder doublet. The underlying flight case is in landing configuration, flaps full, gear down, at 10000 ft with an indicated airspeed of approximately 132 kts, a mass of 47 t and a medium center of gravity location. From handling qualities perspective this flight case is not assumed to be one of the most critical ones, but it is selected as this a flight case for which reference flight data was available. The time histories are provided for all flexible cases depicted in Table 2 and the accelerations due to the respective activated flexible modes are included. The plot order is aligned with the case number, which signifies that whenever different mode cases yielded similar results, the plot for the case with the highest number overlays the others and is visible.



**Fig. 11 Vertical load factor at pilot seat for different combinations of activated modes.**

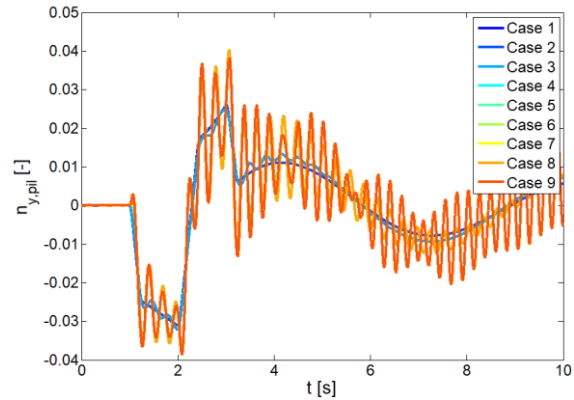


**Fig. 12 Lateral load factor at pilot seat for different combinations of activated modes.**

First of all, significant influences of the flexibility can be observed in both figures. In case of the vertical load factor, the inclusion of the first wing bending mode's dynamics (Case 2) leads to a response which is marginally more sluggish. While adding mode 2 and 3, which are asymmetric modes, hardly has an effect, modes 4 (Case 5) to 8 (Case 9) cause an additional oscillation with relatively low amplitude and high frequency.

The lateral load factor at the captain's seat is influenced by the flexibility in an analogous way. While mode 1 has no visible effect, mode 2 (Case 3), which is asymmetric, adds small oscillations. As shown by the plot for Case 4, mode 3 adds strong higher-frequency oscillations. This mode is an asymmetric fuselage bending and thus leads to lateral displacements at the cockpit. Higher modes do lead to a significantly different behavior any more. The corresponding plots lie above the plot of mode 3. Only mode 8 (Case 9) exhibits slightly different oscillations with slightly higher damping.

## V. Simulator Results

As a last step the flexible aircraft model was implemented in the DLR full motion simulator AVES (Air VEhicle Simulator) [15] and an extensive simulator campaign with pilot-in-the-loop evaluations of the handling qualities of the flexible aircraft was performed. This evaluation is required because the classical handling qualities criteria are designed for rigid-body aircraft and do thus not guarantee to predict deficiencies that arise from the increased flexibility of modern aircraft. The simulator campaign was designed in order to overcome this gap and specifically evaluate the influence of the flexibility on the handling qualities of the aircraft. Details about the setup of the simulator campaign and a description of the different tasks can be found in [17]. The present paper will focus on the synthetic tracking task, in which the pilot has to follow target values of pitch and roll (see Fig. 13) displayed in the PFD as demonstrated in Fig. 14. The flight case is identical to the one used for the times responses in Section IV.

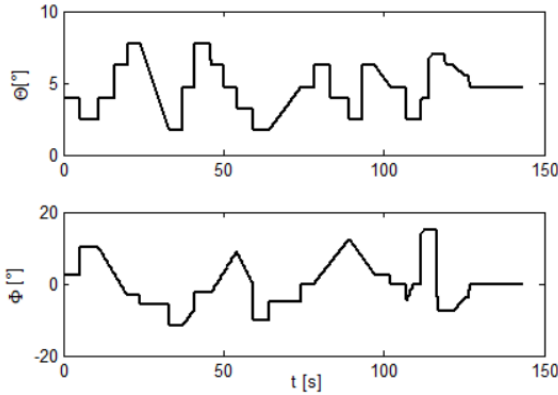


**Fig. 13 Target values for pitch and bank angle of synthetic tracking task.**

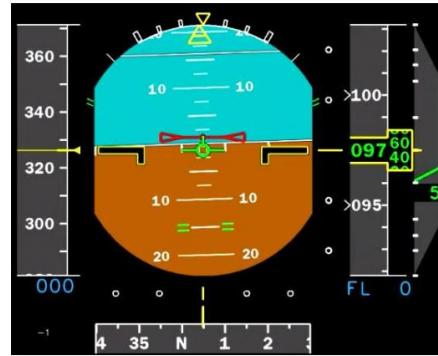
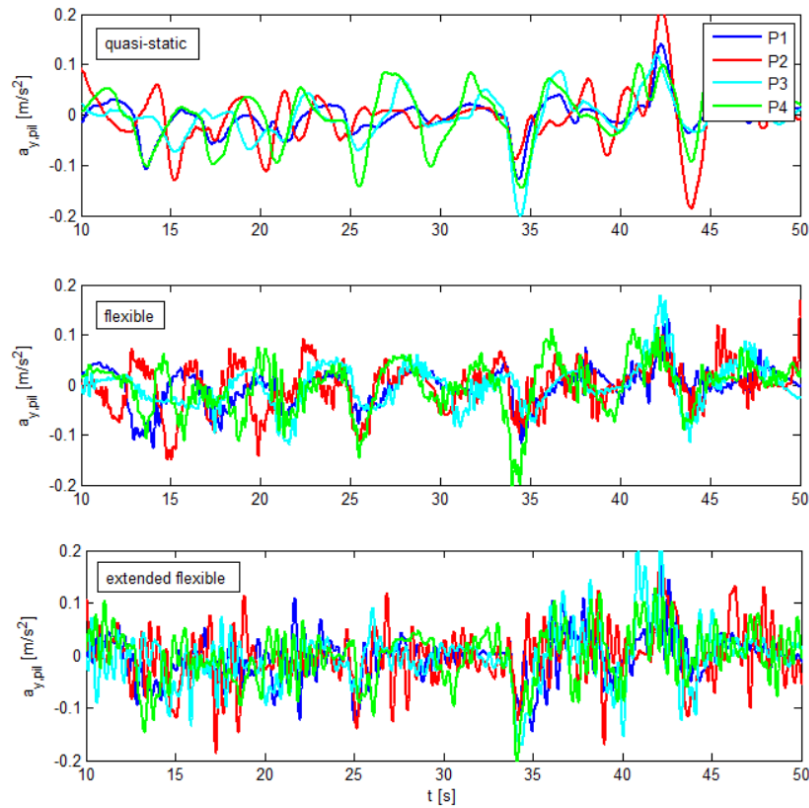


**Fig. 14 Visualization of tracking task with birdy in PFD. [16]**

This task was performed at different flight points (e.g. different speeds, altitudes, weight and balance conditions and flap/gear configurations) with four different Embraer test pilots each. The pilots were asked to give ratings for tendencies towards pilot-induced oscillations (PIOs), for ride comfort and tendencies towards involuntary control input as described in further detail in [17]. For each flight point three different levels of flexibility were tested: a quasi-static implementation of the flexible modes, a flexible model of the aircraft and an aircraft model with extended flexibility. In the quasi-static model all flexible modes are only considered as quasi-static deformation. The flexible model comprises 14 flexible modes, whereupon the first 8 modes are modelled fully dynamically and the remaining 6 modes are quasi-static, which corresponds to the results presented in section F. The model with extended aeroelastic flexibility is realized by the artificial reduction of the structural stiffness described in section C and has the goal to analyze potential future aircraft configurations with higher aeroelastic flexibility. The three models are always tested in the order of increasing flexibility.

Before the actual simulator campaign could be conducted, it had to be assured that the simulator adequately represents the flexible motion of the simulated aircraft. Up to this project, the AVES has only been used to simulate rigid aircraft. Different concepts have been tested to achieve a good representation of the flexible modes by the motion system. Details of these studies can be found in [16]. In the final realization, the accelerations resulting from the flexible modes are not sent into the regular motion cueing algorithm but multiplied by suitable gains and then fed directly to the motion platform. This leads a realistic representation of the flexible modes in ratio to the rigid body modes in the motion simulation and thus assures an accurate impression of the aircraft motion for the pilot.

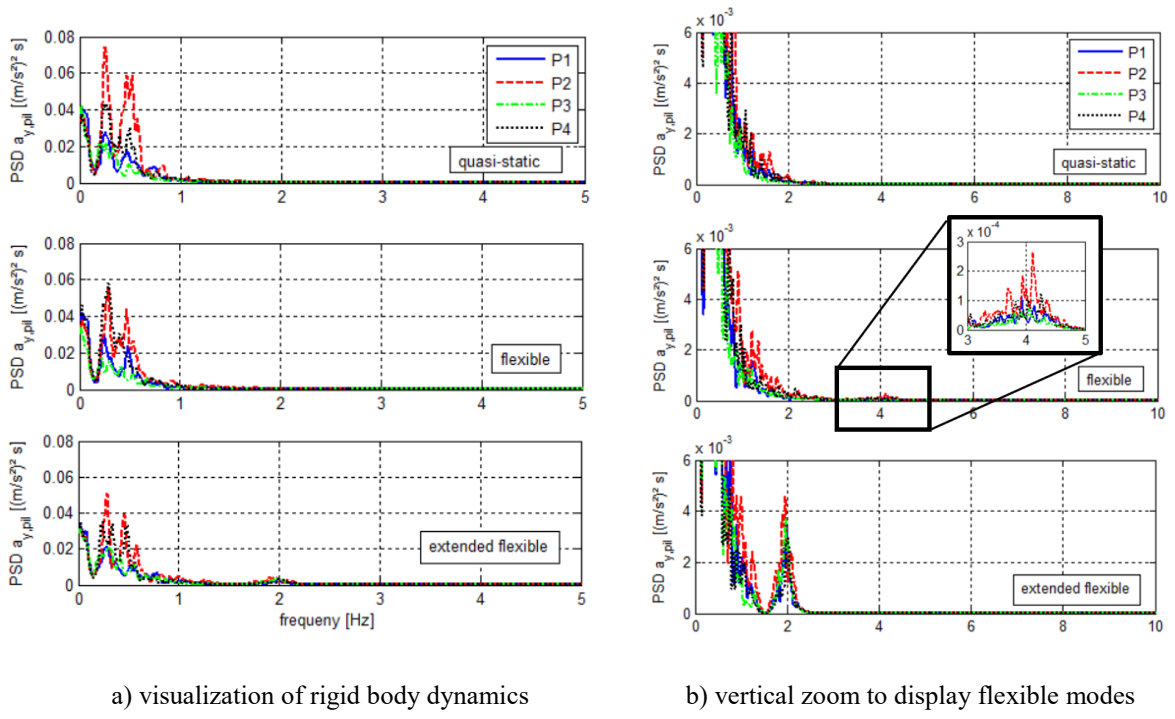
Figure 15 shows the lateral accelerations occurring at the pilot seat during the synthetic task maneuvers performed by four different test pilots with the three different aircraft models. The flight case is identical to section IV. The target values for pitch and roll correspond to the time history shown in Fig. 13 and are therefore identical at each point in time for each task. Due to different pilot's inputs, it cannot be expected that the accelerations are identical, but they are still comparable with respect to their general characteristics. A clear trend of increasing oscillations can be noticed in the lateral accelerations with increasing flexibility. Whereas the upper plot of the quasi-static model only exhibits low-frequency oscillations resulting from pilot inputs to follow the target values of the birdy in the PFD, the lower two plots also show higher frequency oscillations resulting from the flexible aircraft structure. Comparing the lateral accelerations of the flexible model in the middle and the extended flexible model at the bottom, it can be seen that the oscillations increase in amplitude and show a lower frequency, when the structural stiffness is reduced.



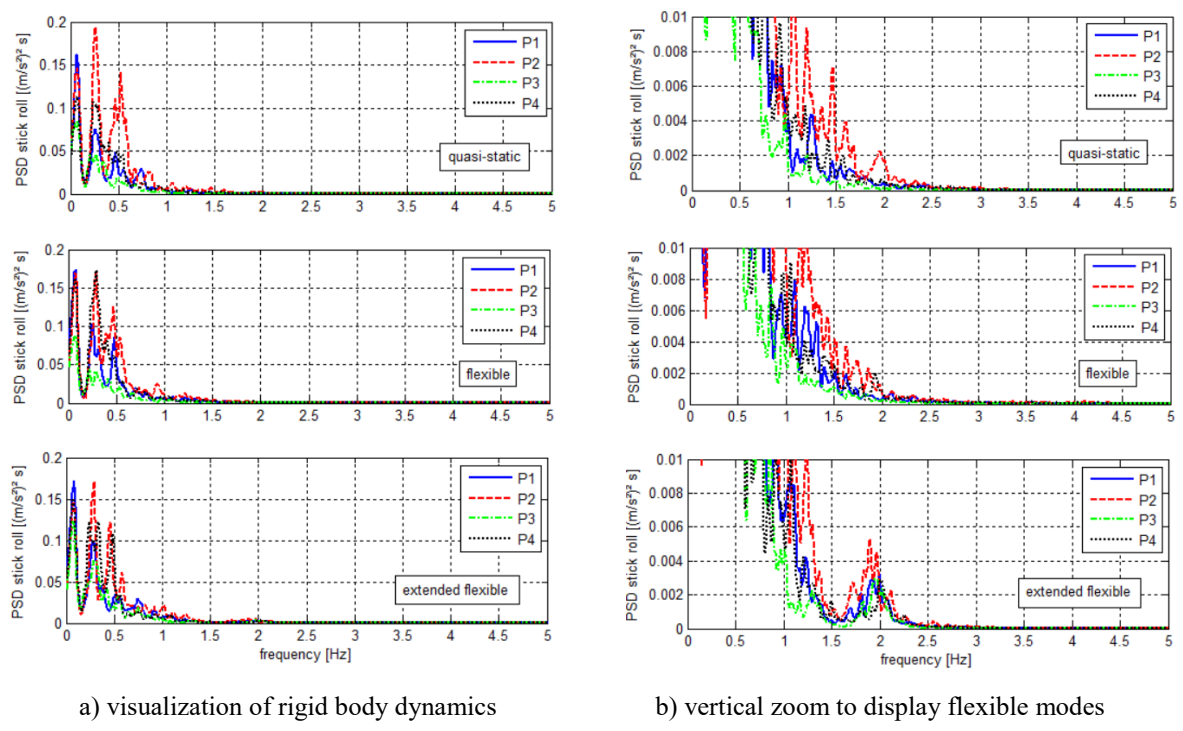
**Fig. 15 Lateral accelerations at pilot seat during synthetic task for quasi-static, flexible and extended flexible model and four different pilots P1 to P4.**

Figure 16 shows the power spectral density (PSD) plot of the translational accelerations at the pilot seat for the entire synthetic task maneuver. Subplots a) on the left-hand side show the rigid body dynamics which occur below 1 Hz and are qualitatively identical for all three flexibility levels. Small differences result from different pilot inputs during the task. For the subplots b) on the right-hand side the y-axis is zoomed in order to display the relevant peaks at the frequencies of the flexible modes. In the quasi-static case at the top, the PSD only shows peaks in the frequency range of the rigid body dynamics displayed in subplot a) on the left-hand side. Above 1 Hz the PSD of the quasi-static model is continuously decreasing without further peaks as no higher-frequency modes are present. In case of the flexible model at the center, a peak occurs at approximately 4 Hz, which corresponds to a flexible mode with a dominant asymmetric fuselage bending. This flexible mode leads to a significant lateral movement of the fuselage and thus a lateral acceleration at the cockpit, which is visible in the PSD here. In case of the extended flexible model, the first flexible mode is reduced and occurs at approximately 2 Hz, which is clearly seen by the peak at 2 Hz in the plot at the bottom.

Figure 17 displays the PSD of the stick inputs in the roll axis. In can be noticed that the pilot reacts to lateral accelerations resulting from the flexible mode at 2 Hz in case of the extended flexible model as there is a peak at 2 Hz. Whether this pilot inputs are intentional pilot commands or involuntary inputs resulting from biodynamic coupling is not definite here and needs further analysis. In case of the flexible model, in contrast, there is no significant peak for the stick inputs around 4 Hz This shows that the higher frequencies and lower amplitude of the flexible modes of the flexible model (compared to the extended flexible model) are significantly less critical for the pilot and do not directly cause significant pilot inputs at frequencies of the flexible aircraft dynamics.



**Fig. 16 PSD of translational accelerations at pilot seat.**



**Fig. 17 PSD of stick inputs in roll axis.**

### G. PIO Assessment

After each task the pilots were asked to provide a PIO rating according to the PIO rating scale given in Fig. 18 and defined in [18]. The resulting ratings of the four test pilots are shown in Fig. 19. It can be noticed that an increasing level of flexibility, by trend leads to increased PIO ratings. The trend is not very strong, as not all pilots reported an increased PIO proneness. Pilot 1 and pilot 4 provided the same PIO rating for all flexibility limits, indicating that their evaluation is based on the rigid body dynamics of the aircraft and not influenced by the structural oscillations. However, pilot 2 and 3 felt a degradation of PIO tendencies with increasing flexibility. Pilot 2 increased the PIO rating from 1 to 2 comparing the flexible model to the quasi-static one. Pilot 3 recognized higher PIO tendencies for the extended flexible model compared to the flexible and quasi-static one.

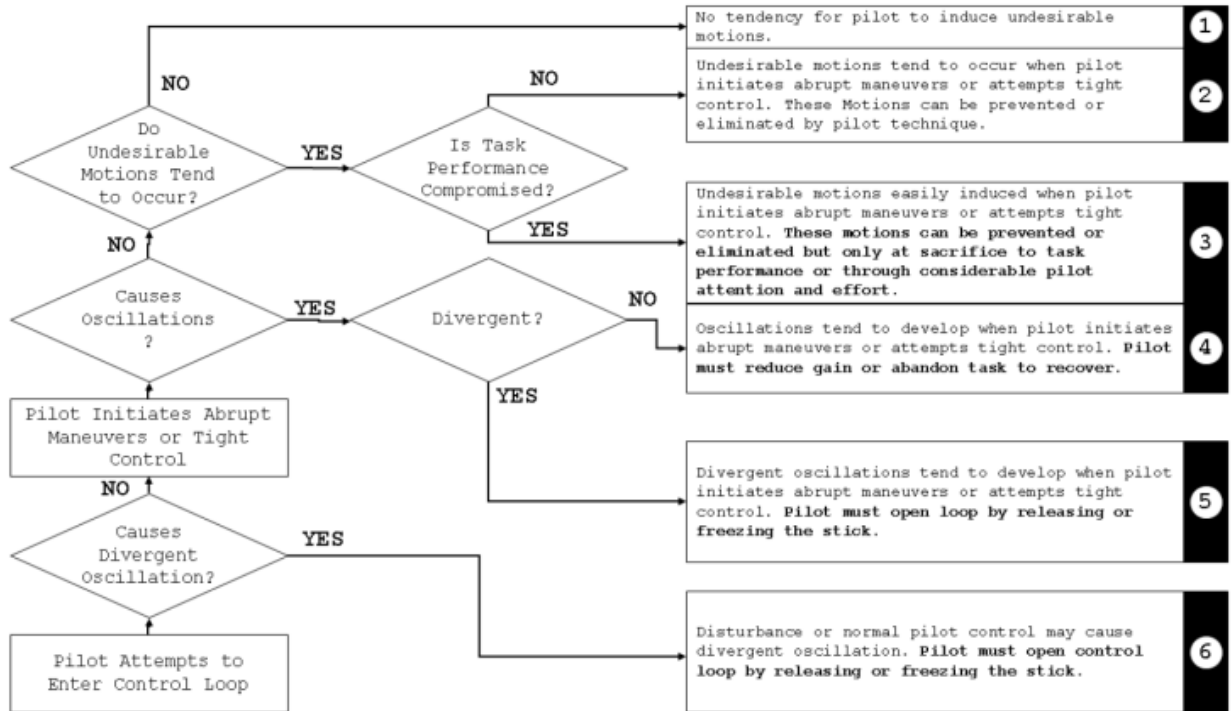


Fig. 18 PIO rating scale [18].

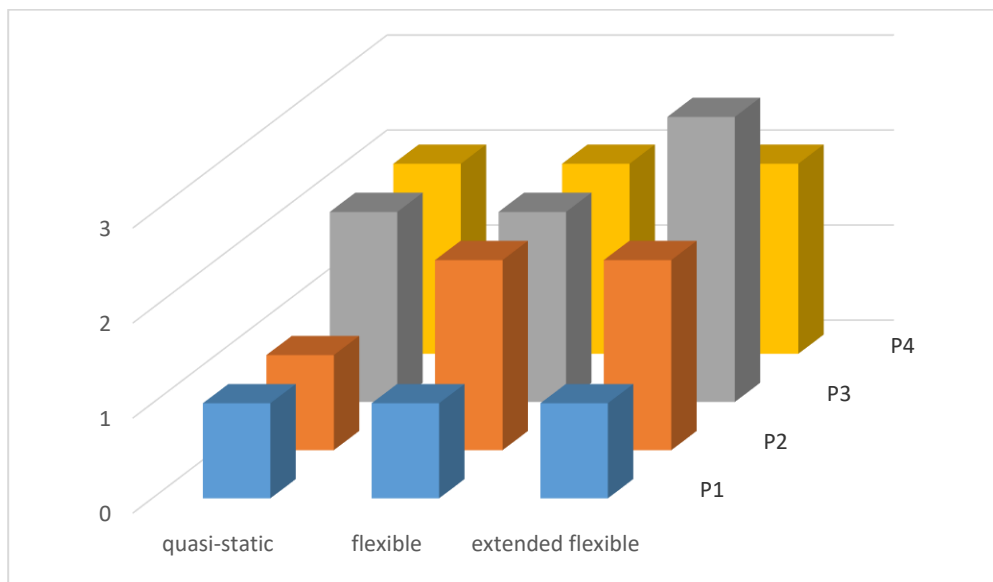


Fig. 19 PIO rating for tracking task.

## H. Ride Comfort

Besides the PIO ratings each task was also assess concerning its ride comfort according to the riding Qualities ratings scale suggested by Raney [19], shown in Table 3.

**Table 3 Riding Qualities Rating (RQR) scale [19].**

Description	Rating
Cockpit vibrations do not impact ride quality	1
Cockpit vibrations are perceptible but not objectionable, no improvement necessary	2
Cockpit vibrations are mildly objectionable, improvement desired	3
Cockpit vibrations are moderately objectionable, improvement warranted	4
Cockpit vibrations are highly objectionable, improvement required	5
Cockpit vibrations cause abandonment of task, improvement required	6

Figure 20 displays the ratings of the four pilots for the tracking task. The diagram shows that pilot 4 felt an increase in the vibration for all three flexibility levels, ranging from no vibrations (RQR 1) for the quasi-static model to mildly objectionable vibrations with improvement desired (RQR 3) for the extended flexible model. Pilot 1 and 3 noticed no impact of vibrations (RQR 1) for the quasi-static and flexible model but light, however not objectionable vibrations (RQR 2) for the extended flexible model. Pilot 2 noticed light, but not objectionable vibrations for all three flexibility levels and rated all cases with an RQR of 2.

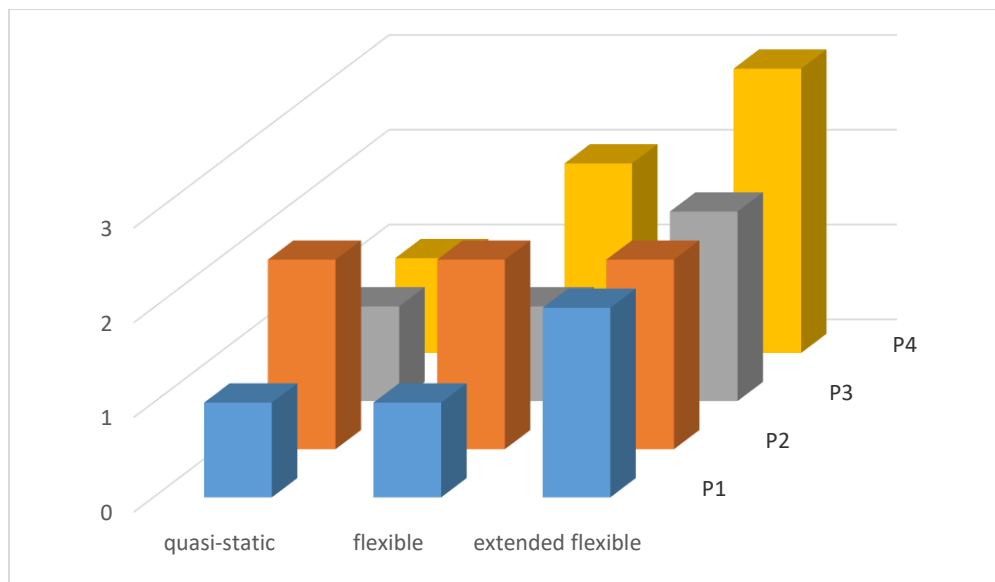


**Fig. 20 Riding qualities ratings for tracking task.**

The ratings are consistent with the time responses of Fig. 15. The increasing level of oscillations is also reflected by the pilot ratings of riding qualities. It is plausible that higher amplitudes of the oscillation in the lateral acceleration at the pilot seat with increasing flexibility level lead to more distinct perception of the vibrations. Moreover, the reduced frequency of the flexible modes of the extended flexibility model further support the objectionable influence of the oscillations as the frequencies are stronger recognizable by the pilot and come closer to the frequencies of the rigid-body modes, which might lead to undesired interferences. This explains that three of four pilots increased their rating for the extended flexibility model.

None of the ratings is larger the 3, suggesting that the ride comfort is not extremely bad. However, a clear trend of worse riding qualities is noticeable with increasing flexibility and the pilots state that improvement is desired.

## VI. Conclusion

The present paper presents a way to enable a handling qualities analysis of modern aircraft with increased structural flexibility. It gives an overview of the development of an aircraft model suitable for the assessment of the influence of structural flexibility on handling qualities as well as first results of the handling qualities assessment itself.

The presented approach for the aircraft model is a low-order aeroelastic model approach and has the advantage of marginal computing time caused by a minimized model complexity on the one hand, and a sufficient reproduction of low-frequency rigid-flexible effects on the other hand. It showed to provide a suitable basis for the system identification applied to given aircraft data. Modal alignment was necessary to investigate the influence of specific mode shapes on the parameter estimation processes and later on in the handling qualities analysis.

The system identification process represents a novel process developed to cope with a limited set of flight test data (with constricted information of local accelerometers) and to generate suitable model for simulator use. The process to iteratively estimate the parameters of the six-degree-of-freedom under the quasi-static deformation and afterwards of the dynamic influence of the flexible modes proved to provide good matches with the flight test data. Even though the structural model parameters were not adjusted and the accelerometers were not weighted during the identification process, an acceptable match could still be achieved for local accelerations as well.

The handling qualities evaluation in the full motion simulator demonstrated that the inclusion of structural flexibility has a noticeable influence on the handling and riding qualities. The increase of structural flexibility led to a perceptible increase in cockpit vibrations and worse pilot ratings up to the level of objectionable vibrations. The influence on the qualities on the PIO proneness on the aircraft was not very strong but recognizable as some pilots provided higher PIO ratings when the flexibility level of the aircraft was higher. Altogether, the pilot simulations in the full motion simulator clearly showed an effect of the flexibility in the aircraft dynamics. The oscillations were evidently noticeable and led to an increased pilot workload, especially in case of the extended flexible model.

In the future, more detailed studies on the effects of aeroelastic flexibility on handling qualities and ride comfort are planned. This includes the assessment of involuntary pilot-induced inputs resulting from high-frequency vibrations, the so-called biodynamic coupling, as well as a more profound analysis of the ride comfort of flexible aircraft. A follow-up project of DLR and Embraer is planned with focus on the development of criteria for the ride comfort particularly for flexible aircraft.

## Acknowledgement

The authors would like to thank the Embraer test pilots for the support during the simulator campaigns. Their fruitful advice during the development of the tasks and simulator setup as well as their evaluations and comments during the campaign itself were very helpful and represent a core part of the handling qualities analysis.

## References

- [1] Ashkenas, I. L., Magdaleno, R. E.; McRuer, D. T., "Flexible aircraft flying and ride qualities"; In: Annual NASA Aircraft Controls Workshop. Hampton, 1983, p. 69-92.
- [2] Waszak, Martin R. and Schmidt, David K.: Flight Dynamics of Aeroelastic Vehicles. Journal of Aircraft, Vol. 25, No. 6, page 563–571, 1988.
- [3] de Oliveira Silva, B. G., Mönnich, W., "System Identification of Flexible Aircraft in Time Domain". AIAA Atmospheric Flight Mechanics Conference, 13-16 August 2012, Minneapolis, Minnesota, USA. DOI: 10.2514/6.2012-4412.
- [4] de Oliveira Silva, B. G., "Data Gathering and Preliminary Results of the System Identification of a Flexible Aircraft Model", AIAA Atmospheric Flight Mechanics Conference, 8-11 August 2011, Portland, Oregon, USA.
- [5] Preisighe Viana, M. V., "Sensor calibration for calculation of loads on a flexible aircraft," 16th International Forum on Aeroelasticity and Structural Dynamics - IFASD 2015, 28 June – 2 July 2015, Saint Petersburg, Russia.
- [6] Preisighe Viana, M. V., "Sensor Calibration for Calculation of Loads on the DLR Discus-2c Sailplane," Tech. Rep. DLR-IB 111-2015/21, Deutsches Zentrum für Luft- und Raumfahrt e.V., 2015. URL <https://elib.dlr.de/99339/>.
- [7] Preisighe Viana, M. V., "Multipoint Model for Flexible Aircraft Loads Monitoring in Real Time: PhD Thesis," Tech. Rep. DLR-FB-2016-66, Deutsches Zentrum für Luft- und Raumfahrt e.V., 2016.
- [8] Preisighe Viana, M. V., "Time-Domain System Identification of Rigid-Body Multipoint Loads Model," Washington, D.C., USA, 2016. doi:10.2514/6.2016-3706.
- [9] de Oliveira Silva, B. G., "System Identification of Flexible Aircraft in Time Domain: PhD Thesis," Tech. Rep. DLR-FB-2018-29, Deutsches Zentrum für Luft- und Raumfahrt e.V.

- [10] Mönnich, W.: Ein 2-Punkt-Aerodynamikmodell für die Identifizierung. Systemidentifikation in der Fahrzeugdynamik: Symposium des Sonderforschungsbereiches SFB 212 "Sicherheit im Luftverkehr", in German, Braunschweig, March 10-11 1987.
- [11] Jategaonkar, R., Identification of the Aerodynamic Model of the DLR Research Aircraft ATTAS from Flight Test Data, Deutsche Forschungsanstalt für Luft- und Raumfahrt e. V. (DLR), Cologne, Germany, 1990.
- [12] Dykman, J. R., Rodden, W. P., "Structural Dynamics and Quasistatic Aeroelastic Equations of Motion", Journal of Aircraft, Vol. 37, No. 3, May 2012, pp. 538-542, DOI: 10.2514/2.2634.
- [13] Allemang, R. J., "The Modal Assurance Criterion – Twenty Years of Use and Abuse", Sound and Vibration, August 2023.
- [14] Jategaonkar, R. V., Flight Vehicle System Identification - A Time Domain Methodology, 2nd ed., Progress in Astronautics and Aeronautics, Vol. 245, American Institute of Aeronautics and Astronautics, Inc., 1801 Alexander Bell Drive, Reston, Virginia 20191, USA, 2015.
- [15] Duda, H., Gerlach, T., Advani, S., Potter, M., "Design of the DLR AVES Research Simulator", AIAA Modeling and Simulation Technologies (MST) Conference, Boston, MA, 19-22 Aug. 2013, DOI: 10.2514/6.2013-4737.
- [16] Schwithal, J., Buch, J.-P., Seehof, C., Drewiacki, D., Moreira, F. J. O., "Simulating Flexible Aircraft in a Full Motion Simulator", AIAA AVIATION 2023 Forum, 12-16 June 2023, San Diego, CA and Online.
- [17] Moreira, F. J. O., Drewiacki, D., Marco Antônio de O. Alves, M. A., Buch, J.-P., Schwithal, J., Seehof, "Flight Simulator Result Comparing Three Aircraft Configurations: Quasi-Static, Flexible and Extended Flexibility", AIAA SciTech Forum, National Harbor, MD & Online, 23-27 January 2023, DOI: 10.2514/6.2023-1368.
- [18] Mc Ruer, D. T., Pilot-Induced Oscillations and Human Dynamic Behaviour", NASA-CR-4683, July 1995.
- [19] Raney, D. L. et al, "The impact of structural vibration on flying qualities of a supersonic aircraft", AIAA Atmospheric Flight Mechanics Conference and Exhibit. Montreal, 2001, AIAA 2001-4006.